Supporting Information

Hybrid Multilayered Plasmonic Nanostars for Coherent Random Lasing

Battulga Munkhbat[1], Johannes Ziegler[1], Hannes Pöhl[1], Christian Wörister,[1] Dmitry Sivun[1], Markus C. Scharber[2], Thomas A. Klar[1], and Calin Hrelescu[1*]

1. Institute of Applied Physics, Johannes Kepler University Linz, 4040 Linz, Austria

2. Linz Institute for Organic Solar Cells / Institute of Physical Chemistry, Johannes Kepler University Linz, 4040 Linz, Austria

e-mail: calin.hrelescu@jku.at

Characterization of Hybrid Multilayered Plasmonic Nanostars

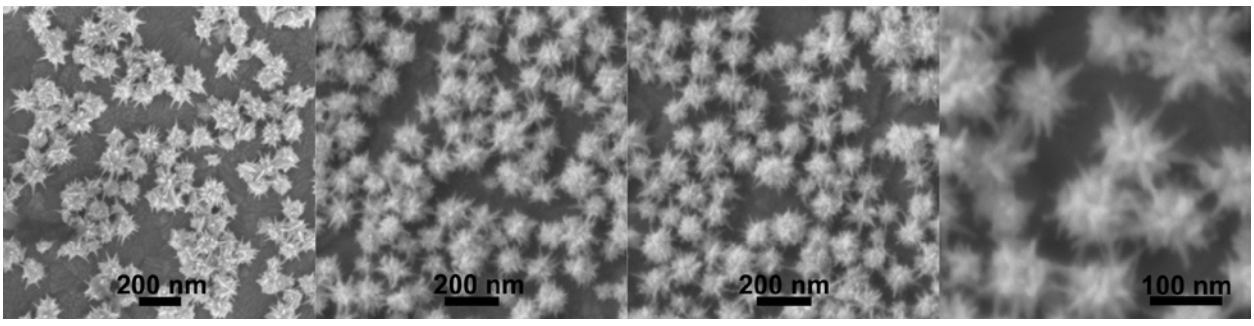

Figure S1. Zoomed-out SEM images of representative gold nanostars (AuNSts) stemming from three different synthesis batches.

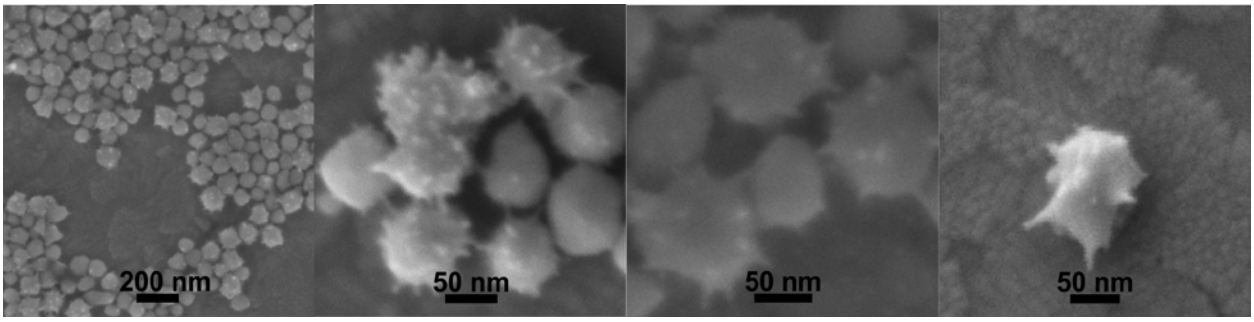

Figure S2. SEM images of representative silver-enhanced gold nanostars (AuAgNSts) stemming from three different synthesis batches.

Scanning TEM (STEM) was performed with a bright field (BF) and a high angle annular dark field (HAADF) detectors. Elemental line and mapping analysis were carried out using energy dispersive X-ray spectroscopy (EDX). The samples were investigated with a JEOL JEM-2200FS transmission electron microscope in STEM mode operated at 200kV, equipped with an Oxford SDD X-maxN (80 mm^2) EDX-system. (see Figure S3)

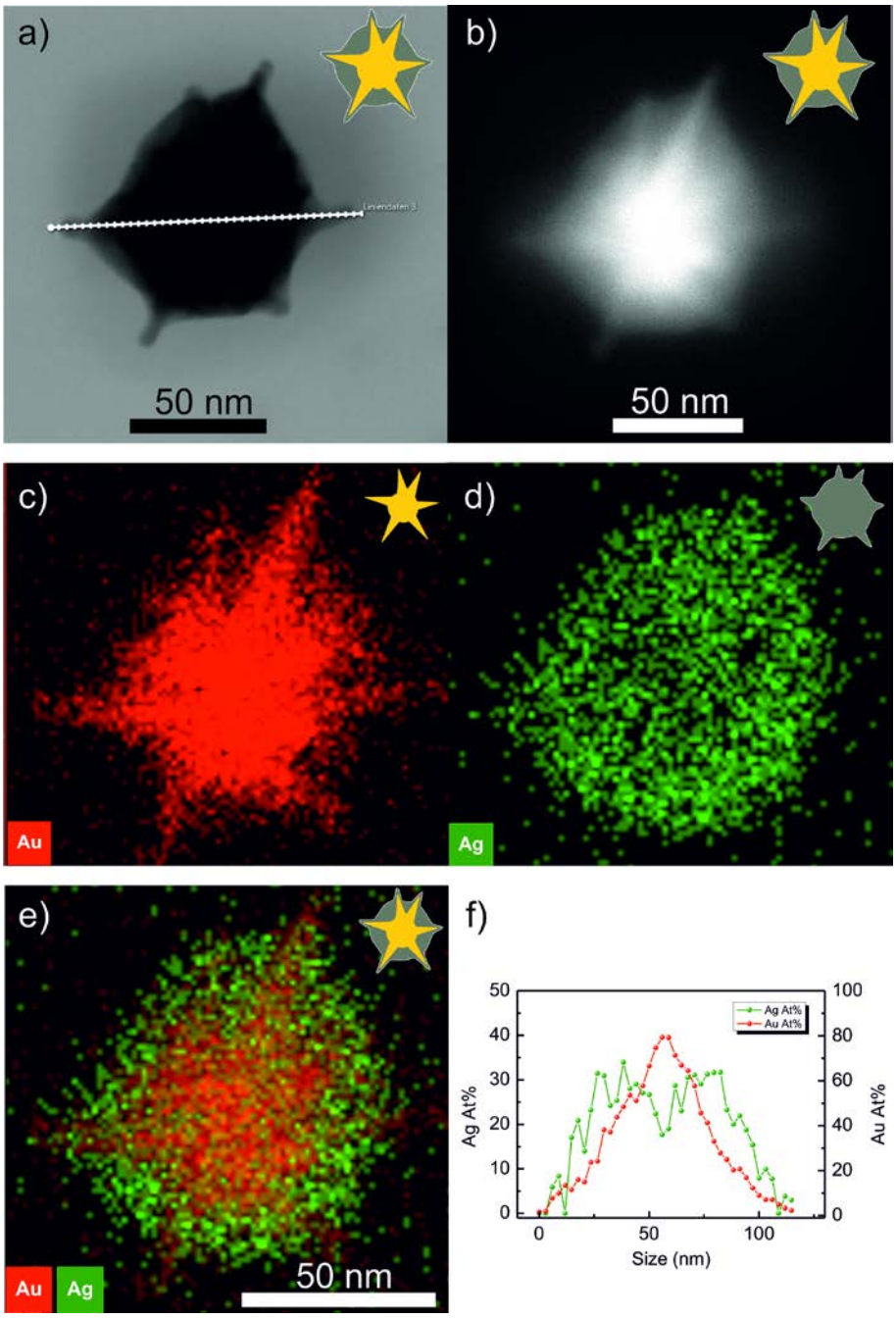

Figure S3. (a) STEM image of a representative AuAgNSt, (b) HAADF-STEM image of the same AuAgNSt, (c-d) STEM-EDX individual elemental maps of (c) Au and (d) Ag distribution. (e) Superposition of the individual elemental maps for Au (red) and Ag (green) in the AuAgNSt. (f) Elemental line analysis of the Au and Ag content in the AuAgNSt. The trace for the line analysis is illustrated as white line in (a). The AuAgNSts are layered nanostructures, with a star shaped gold core and a star shaped silver shell.

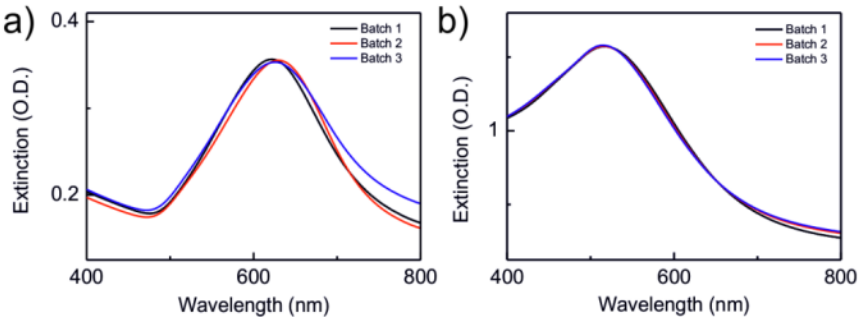

Figure S4. Reproducibility of the AuNSts and AuAgNSts synthesis: Extinction spectra of three different synthesis batches (a) of AuNSts and (b) of AuAgNSts. Negligible batch to batch variations in the optical ensemble spectra are achieved for the AuNSts. After the silver-enhancement of the respective nanostars, nearly no batch to batch variations in the optical ensemble spectra could be observed for the AuAgNSts dispersed in ethanol.

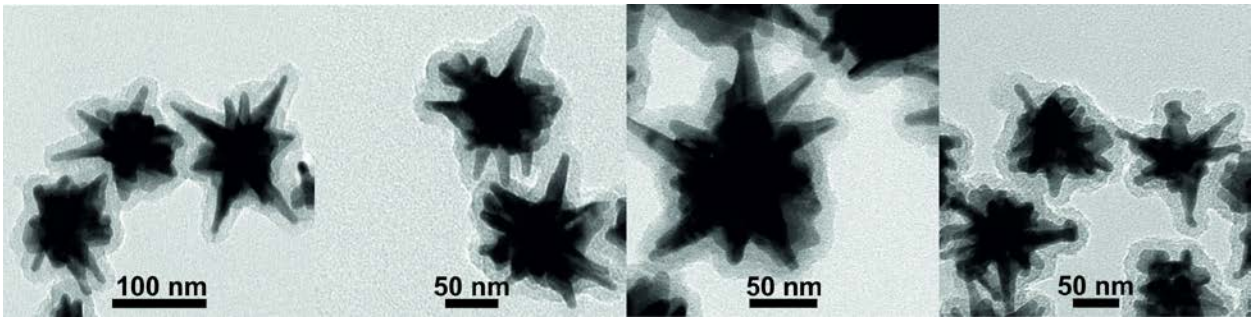

Figure S5. Zoomed-in TEM images of representative silica coated gold nanostars (AuNSts@SiO_2) stemming from three different synthesis batches.

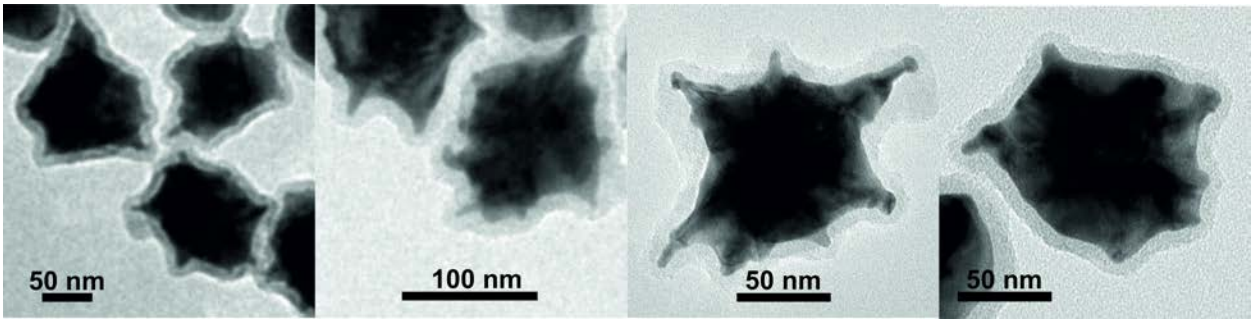

Figure S6. TEM images of representative silica coated silver-enhanced gold nanostars (AuAgNSts@SiO_2) stemming from three different synthesis batches.

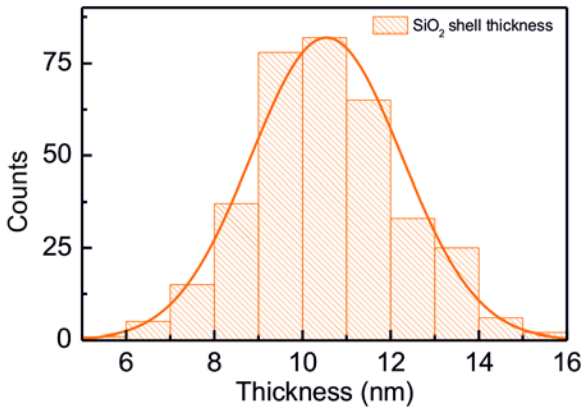

Figure S7. Histogram of the silica shell thickness. 70 particles were analyzed manually with the free software Gwyddion.[1] For each particle, the silica shell thickness was measured at 4 - 5 different locations to analyze the homogeneity of the silica shell.

In the random lasing experiments the position of the cuvette containing the gain-nanostars solutions is fixed, and the solutions are not stirred. Typically, the experiments for each sample are completed in less than an half an hour. Precipitation and aggregation of the nanostars in the gain-nanostar solutions is avoided by the silica shell or with thiolated mPEG functionalization of the nanostars. In Figure S8, extinction spectra of AuAgNSts with and without silica shell dispersed in ethanol are shown. The spectra were recorded every hour. The AuAgNSts and AuAgNSts@SiO_2 dispersed in ethanol did not show any significant change in optical density (OD) during the period of 10 hours. Furthermore, there was no significant change in the shape of extinction spectra of both multilayered nanostars. This implies that no significant precipitation or aggregation of the AuAgNSts with and without silica shell occurs over a monitoring period of ten hours without stirring, which is substantially longer than the time needed to complete the random lasing experiments for one sample.

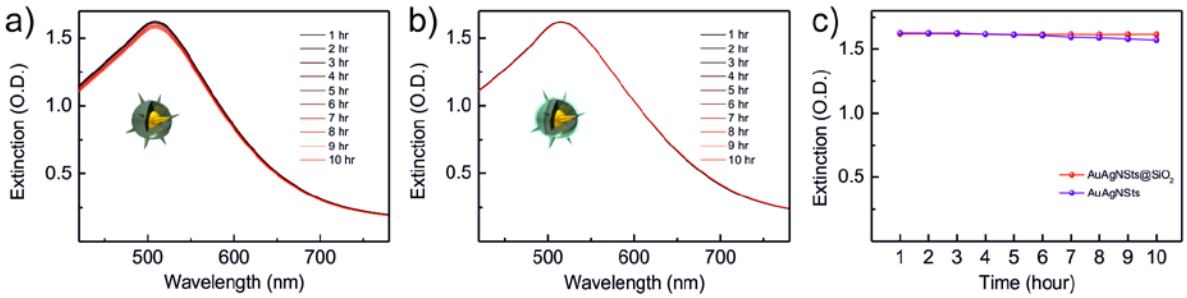

Figure S8. Extinction spectra of a) AuAgNSts and b) AuAgNSts@SiO_2 in ethanol recorded every hour for a period of 10 hours. The solutions containing nanostars are not stirred or shaken during the period of 10 hours. c) The optical densities (OD) at the extinction maximum of both AuAgNSts and AuAgNSts@SiO_2 dispersions do not show any significant change during the 10 hours without stirring.

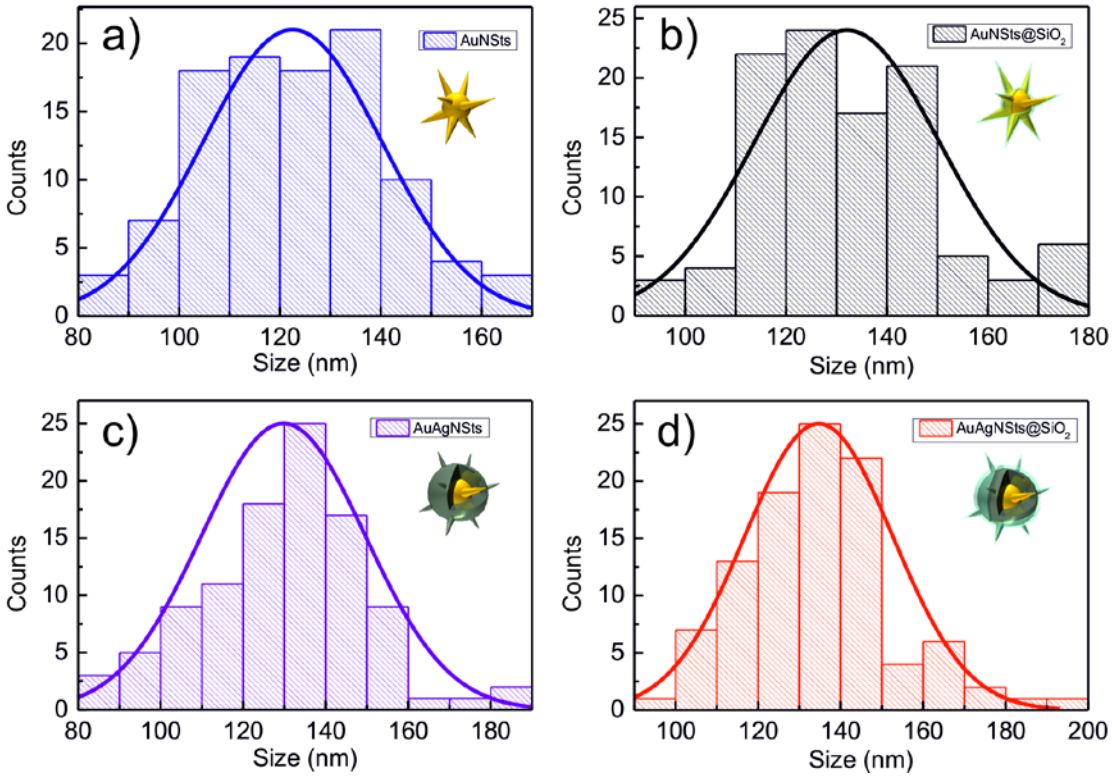

Figure S9. Histograms of the tip-to-tip diameters of a) AuNSts, b) AuNSts@SiO_2, c) AuAgNSts and d) AuAgNSts@SiO_2. For each type of the nanostars, the tip-to-tip diameters were measured manually with Gwyddion[1] for 30 particles. For each particle 3 - 4 tip-to-tip distances between different tips were considered.

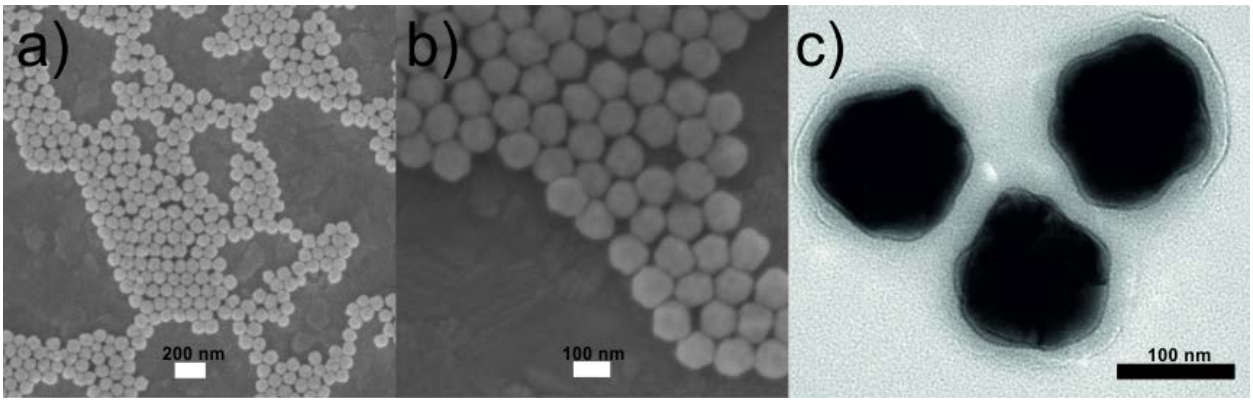

Figure S10. SEM images of the citrate-capped spherical gold nanoparticles (125 nm in diameter) were purchased from Nanopartz (left and middle) and TEM image of representative silica coated spherical gold nanoparticles (right).

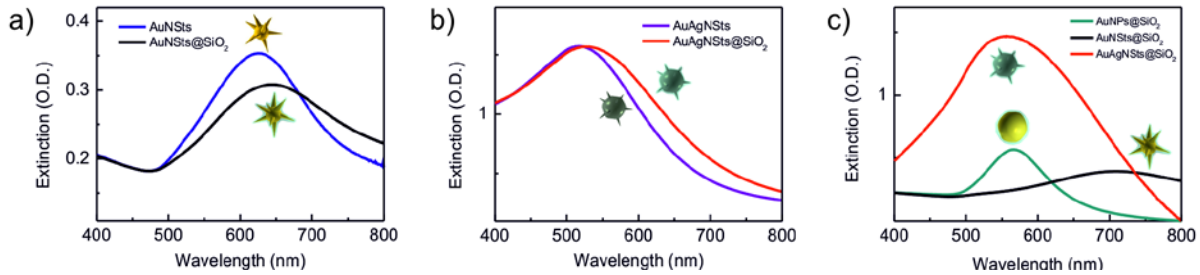

Figure S11. (a) Extinction spectra of AuNSts and AuNSts@SiO_2 in ethanol. The concentration of AuNSts and AuNSts@SiO_2 was adjusted in such a way that both dispersions have the same optical density at 405 nm. (b) Extinction spectra of AuAgNSts and AuAgNSts@SiO_2 in ethanol. The AuAgNSts and AuAgNSts@SiO_2 were directly synthesized out of a part of the AuNSts, so that the concentrations are considered to be similar. Due to the silver enhancement the AuAgNSts and AuAgNSts@SiO_2 in ethanol exhibit a ~4 times higher extinction as the AuNSts**.** (c) Extinction spectra of AuNSts@SiO_2, AuAgNSts@SiO_2 and AuNPs@SiO_2 in chlorobenzene.

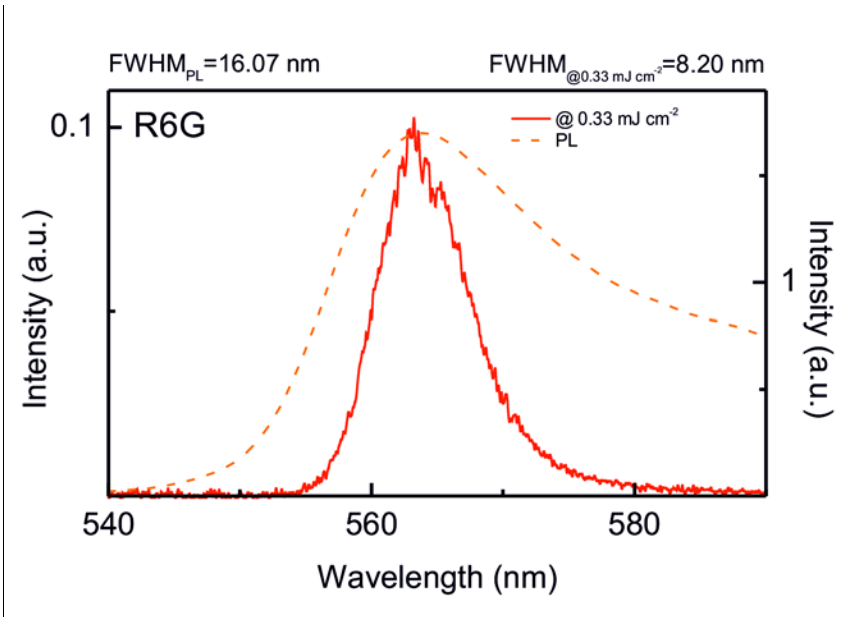

Figure S12. The emission spectrum of the reference R6G solution shows amplified spontaneous emission (ASE) with a substantially reduced spectral bandwidth (continuous red curve with full width half maxima of $FWHM_{@0.33=}$8.20 nm) for fluences above 0.30 mJ cm^{-2} compared to PL (dashed curve with a $FWHM_{PL}$=16.53 nm).

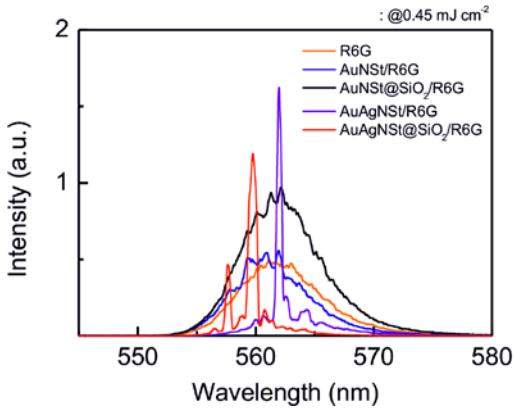

Figure S13. Emission (random lasing or ASE) spectra at an excitation fluence of 0.45 mJ cm^{-2} for nanostars/R6G mixtures. Surprisingly, no pronounced ASE background is detected even at low pumping fluences in contrast to the previously mentioned samples.

Combined dark-field and random lasing experiments supported by accurate theoretical modeling might allow deeper insights in the ASE-suppression mechanism.[2,3]

Numerical Modelling of hybrid multilayered plasmonic nanostars

In order to underline our experimental findings on the optical properties of the hybrid multilayered nanostars, three-dimensional finite difference time domain (FDTD) calculations were performed. We used the commercially available FDTD solver (version 8.9.269) from Lumerical Solutions Inc. to calculate the field enhancement distributions and scattering cross sections of hybrid multilayered nanostars. Since the investigation of the exact properties of specific hybrid multilayered nanostars and their individual plasmonic resonances includes vast numerical calculations and lots of detailed numerical modelling as well as detailed analysis and experiments at the single particle level, which are beyond the scope of this manuscript, we restricted ourselves to a simpler model in order to mimic the key plasmonic properties of the hybrid multilayered nanostars for coherent random lasing best as possible, namely their scattering cross-section and the field enhancement distributions. The gold nanostars were emulated as gold-spheres (80 nm in diameter) as the nanostar's core, from which five tips are protruding in the same plane, but pointing in arbitrary directions, avoiding the formation of any symmetry. The tips are modeled as rounded cones with a tip curvature of 8 nm. The individual tip length was chosen between 20 and 30 nm so that the maximal apex-to-apex distance is 120 nm, similar to the real nanostars. The cone opening angle was set to 40°, since for these modelling parameters the spectral position of calculated plasmon resonances agrees reasonably good with the spectral position of the observed main extinction maxima. The silver shell (thickness S_{Core}) and the silica shell (with a fixed thickness of 10 nm) around the gold core were modeled by concentric spheres of the corresponding material with bigger diameter. The silver shell (with a variable thickness S_{Tip}) and the silica shell (with a fixed thickness of 10 nm) around the tips were modeled by adding symmetrically enlarged rounded cones around the corresponding tips in order to achieve core-shell-shell tips with a common symmetry axis. In the modeling, the permittivity of gold and silver was obtained by a generalized multi-coefficient fit of the permittivity of bulk gold and silver according to Johnson and Christy.[4]

The calculations were performed for nanostars dispersed in ethanol (refractive index of 1.36). For the silica shell, a refractive index of 1.39 was used, which is typical for a TEOS thin layer in ethanol.[5] The Total Field/Scattered Field (TFSF) source implemented in the software was used as excitation source, emitting a plane wave with the same spectral bandwidth as in the extinction experiments. The excitation direction was vertical to the common plane of the five tips.

Figure S14 shows the calculated scattering cross sections for a single AuNSt (black), for the same AuNSt coated with a homogenous 10 nm Silica (TEOS) layer as model for the AuNSt@SiO_2, for the AuAgNSt (same AuNSt covered with Ag with a thicknesses of S_{Tip}= 8 nm and S_{core}= 20 nm, typical for the AuAgNSts in the experiments) and the model AuAgNSt@SiO_2, which is the same AuAgNSt, additionally covered with a 10 nm silica shell.

The experimental findings are qualitatively reproduced by the simulations. Upon silica-coating, the calculated plasmon resonances of the AuNSts redshift due to the introduction of a

higher refractive index medium around the AuNSts compared to the background refractive index. Additionally, besides the spectral redshift, the silica shell induces a spectral broadening of the plasmon resonances. It should be pointed out that the experimental extinction spectra, which were measured on an ensemble, are the superposition of all extinction spectra of individual nanostars. Since every individual nanostar possesses a nearly unique morphology, which determines the number and spectral position of the multiple plasmon resonances, it is nearly impossible to achieve a perfect quantitative agreement between calculated spectra of individual nanostars and the experimental ensemble extinction.

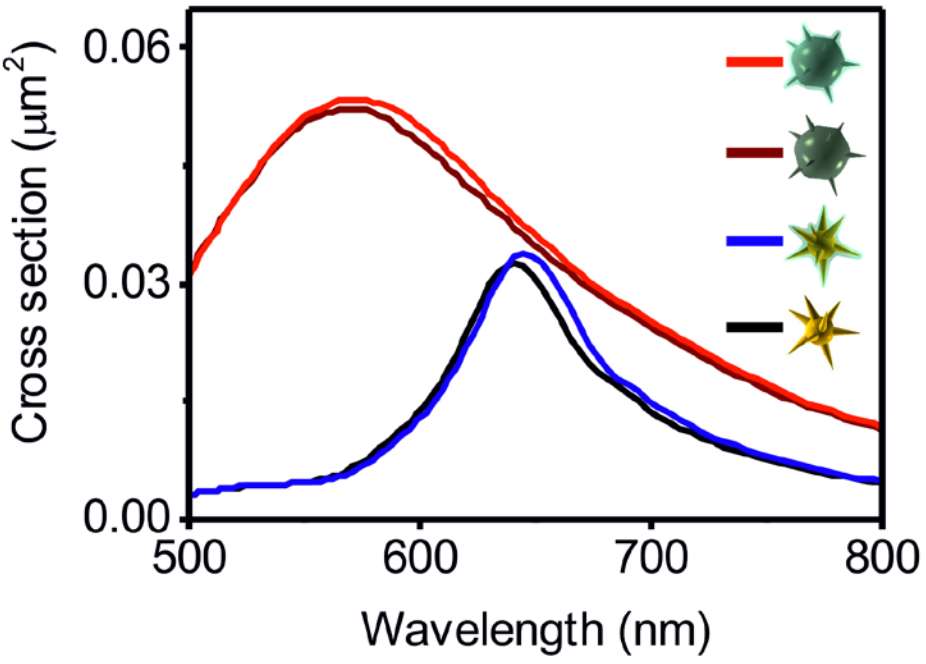

Figure S14. Calculated scattering cross sections for the same single gold nanostar with different coatings, pure AuNSt, AuNSt@SiO_2, AuAgNSt and AuAgNSt@SiO_2.

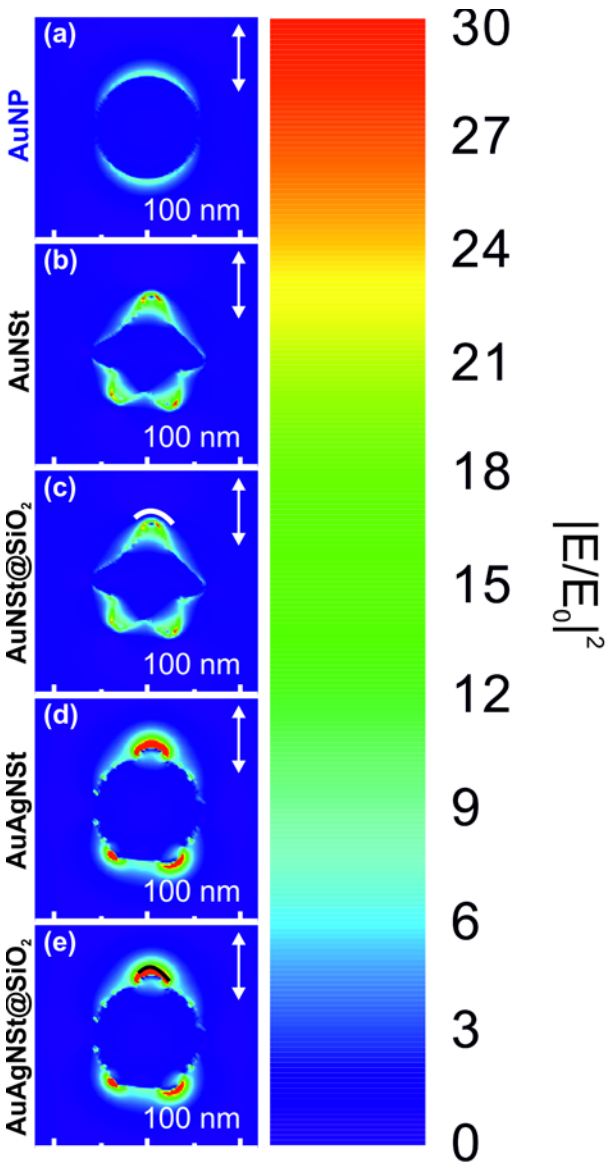

Figure S15. Calculated intensity enhancement distribution $\left|\frac{E}{E_0}\right|^2$ at the pump excitation wavelength (532 nm). The incident excitation polarization is indicated by the white double arrow. (a) for a spherical AuNP, and the nanostars with scattering cross sections displayed in Figure S14, (b) AuNSt, (c) AuNSt@SiO_2 (white curve indicates the SiO_2 shell), (d) AuAgNSt and (e) AuAgNSt@SiO_2 (black curve indicates the SiO_2 shell).

An example of the influence of the silver shell thickness on the plasmon resonances of single AuNSt, i.e. the scattering cross section, is illustrated in **Figure S16**. In all calculations, the AuNSt, the excitation polarization and the surrounding medium of the AuNSt are kept constant.

The growth of the silver shell is modeled assuming that the Ag shell thickness around the core S_{core} increases from 8 to 20 nm, while the Ag shell on the tips of the AuNSt remains constant at S_{Tip}= 8 nm. Already with an 8 nm thick silver shell on the core and tips of the AuNSt, the scattering cross section of the AuAgNSt (red curve) is blue shifted and increased with respect to the scattering cross section of a AuNSt (black curve). With increasing $S_{core,}$ the plasmon resonances of the AuAgNSts blue shift further and the scattering cross section increases, as was also observed experimentally and was calculated by Fales et al.[6]

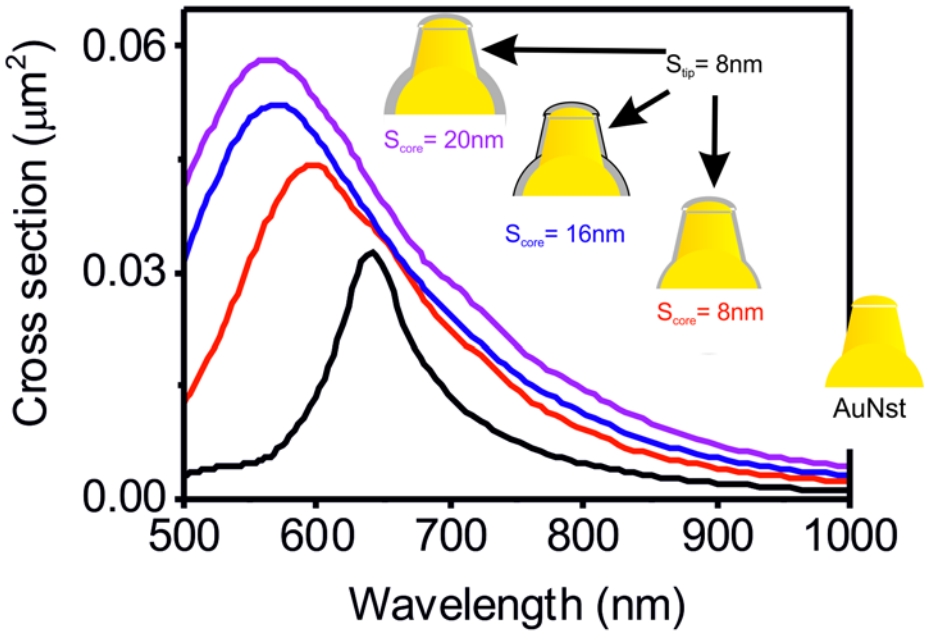

Figure S16. Calculated scattering cross section for a AuNSt (black) and AuAgNSt with different Ag shell thickness S_{core} (8 nm, 16 nm, and 20 nm) around the gold core, but a constant Ag shell thickness of 8 nm on the tips gold tips.

Random lasing of MEH-PPV

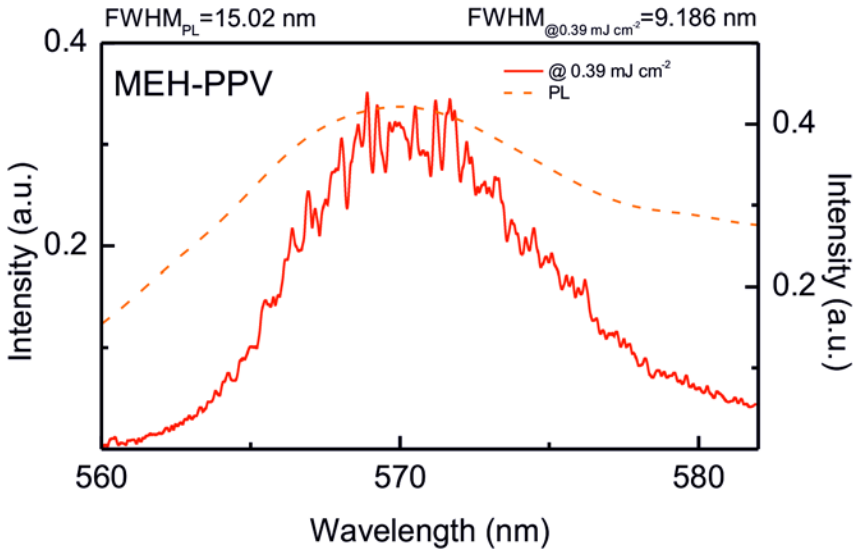

Figure S17. The emission spectrum of the reference MEH-PPV solution shows amplified spontaneous emission (ASE) with a reduced spectral bandwidth (continuous red curve with full width half maxima of $FWHM_{@0.39}$=9.18 nm) for fluences above 0.30 mJ cm^{-2} compared to PL (dashed curve with a $FWHM_{PL}$=15.02 nm).

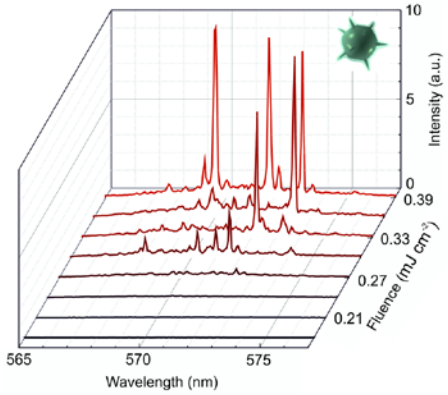

Figure S18. Detail of random lasing emission spectra of MEH-PPV with AuAgNSts@SiO_2.

(1) Department of Nanometrology, Czech Metrology Institute, Gwyddion – Free SPM (AFM, SNOM/NSOM, STM, MFM) Data Analysis Software, 2015.
(2) Arnold, N.; Ding, B.; Hrelescu, C.; Klar, T. A. Dye-Doped Spheres with Plasmonic Semi-Shells: Lasing Modes and Scattering at Realistic Gain Levels. Beilstein J. Nanotechnol. **2013**, 4, 974–987.
(3) Arnold, N.; Hrelescu, C.; Klar, T. A. Minimal Spaser Threshold within Electrodynamic Framework: Shape, Size and Modes. Ann. Phys. **2016**, 528 , 295–306.
(4) Johnson, P. B.; Christy, R. W. Optical Constants of the Noble Metals. Phys. Rev. B **1972**, 6 (12), 4370–4379.
(5) Holowacz, I.; Podbielska, H.; Bauer, J.; Ulatowska-Jarza, A. Viscosity, Surface Tension and Refractive Index of Tetraethylorthosilicate-Based Sol-Gel Materials Depending on Ethanol Content. Opt. Appl. **2005**, 35, 691–699.
(6) Fales, A. M.; Yuan, H.; Vo-Dinh, T. Development of Hybrid Silver-Coated Gold Nanostars for Non-Aggregated Surface-Enhanced Raman Scattering. J. Phys. Chem. C **2014**, 118, 3708–3715.